Electrical Power and Energy Systems 55 (2014) 1–12

Contents lists available at ScienceDirect

Electrical Power and Energy Systems

journal homepage: www.elsevier.com/locate/ijepes

Optimizing reactive power flow of HVDC systems using genetic algorithm

Ulaş Kılıç [a,*], Kürşat Ayan [b], Uğur Arifoğlu [c]

[a] Department of Mechatronics Engineering, Celal Bayar Universirty, Manisa, Turkey
[b] Department of Computer Engineering, Sakarya University, Sakarya, Turkey
[c] Department of Electrical-Electronics Engineering, Sakarya University, Sakarya, Turkey

ARTICLE INFO

Article history:
Received 2 August 2012
Received in revised form 16 July 2013
Accepted 8 August 2013

Keywords:
Optimal reactive power flow
Integrated AC–DC system
Heuristic method
Genetic algorithm
Evolutionary

ABSTRACT

Due to the usage of high voltage direct current (HVDC) transmission links extensively in recent years, it requires more studies in this issue. Two-terminal HVDC transmission link is one of most important elements in electrical power systems. Generally, the representation of HVDC link is simplified for optimal reactive power flow (ORPF) studies in power systems. ORPF problem of purely AC power systems is defined as minimization of power loss under equality and inequality constraints. Hence, ORPF problem of integrated AC–DC power systems is extended to incorporate HVDC links taking into consideration power transfer control characteristics. In this paper, this problem is solved by genetic algorithm (GA) that is an evolutionary-based heuristic algorithm for the first time. The proposed method is tested on the modified IEEE 14-bus test system, the modified IEEE 30-bus test system, and the modified New England 39-bus test system. The validity, the efficiency, and effectiveness of the proposed method are shown by comparing the obtained results with that reported in literature. Thus, the impact of DC transmission links on the whole power systems is shown.

1. Introduction

ORPF is an energy system problem that the scientists try to solve for a long time [1–5]. The problem is minimization of the power loss in an energy network. In other words, the aim is minimization of objective function which is power loss in an energy system. At the same time, the objective function of whole system is minimized under equality and inequality constraints. The equality and inequality constraints in purely AC system are power equalities defined for all the buses and physical constraints of the energy system, respectively. All the constraints have been to be satisfied while the power loss of whole the system is being minimized.

The scientists have used many different methods for solving ORPF problem of purely AC power systems [1–13]. These methods are numerical and heuristic methods. According to the results reported in literature, it can be seen that heuristic methods are superior from the numerical methods [4–13]. One important advantage of heuristic methods is that they convergence to the optimum solution in shorter time than others and without reaching local minimums.

Because of the energy consumption increasing rapidly in recent years, it is required to increase the power generation capacity. This causes to over load the transmission lines. Thus, even small perturbations can cause a part of the energy system to leave the synchronization even if it is subjected to the small perturbations. It is needed to reschedule energy systems to avoid such undesirable situations like these and to maintain the continuity of the operating. So in recent years, the power system planners try to reschedule the energy systems to transfer the power through HVDC links in recent years. There are many advantages of the power transmission through HVDC links. For examples, reactive power is not transferred through HVDC links and energy loss of HVDC links is lesser than long AC system transmission lines. Additionally, the instantaneous power in neighboring AC systems can be controlled by HVDC links. Furthermore, HVDC links is used to stabilize electric power systems [14]. Recently, many researches are performed on realization of HVDC models for power flows studies [15–19]. The formulation for the basic model of two-terminal HVDC link is given in Ref. [20].

In ORPF problem of the integrated AC–DC power systems, DC link constraints are included in the problem. In the literature, there are two basic approaches for solving the power flow equations. The first is the sequential approach [19,21,22]. In this method, AC and DC equations are solved separately by successive iterations. Although the implementation of the sequential method is simple, it has convergence problems associated with certain situations.

* Corresponding author. Address: Department of Mechatronics Engineering, Celal Bayar Universirty, Manisa, Turkey. Tel./fax: +90 236 314 10 10

E-mail addresses: ulas.kilic@cbu.edu.tr (U. Kılıç), kayan@sakarya.edu.tr (K. Ayan), arifoglu@sakarya.edu.tr (U. Arifoğlu).

0142-0615/$ - see front matter
http://dx.doi.org/10.1016/j.ijepes.2013.08.006

Furthermore the state vector does not contain explicitly DC variables. The second approach is known as the unified approach [23]. In this study, the first method is used.

GA is a heuristic algorithm based on native selection. The basic logic of this algorithm is based on the living of strong individuals in nature and the dying of others. This algorithm consists of stages as initial population, fitness scaling, selection, crossover, mutation and stopping. GA has been used successfully for solution of the engineering problem for a long time [24–29]. In this paper, GA is used for solution of ORPF problem in integrated AC–DC power systems for the first time.

After this introduction, the modeling of DC transmission link is represented in Section 2. The methodology of GA is explained in Section 3. GA based optimal reactive power flow solution of HVDC systems is explained in Section 4. In order to demonstrate validity, efficiency and effectiveness of the proposed method, simulation results of the modified IEEE 14-bus test system, the modified IEEE 30-bus test system and the modified New England 39-bus test system are given and the obtained results are extensively evaluated and compared to that reported in the literature in section 5. Finally, the conclusions are discussed in section 6.

2. The modeling of DC transmission link

Before analyzing DC transmission system, it is necessary to model DC transmission link and the converters. The modeling is made based on accepted assumptions in the literature. The assumptions are as follows [23]:

- The main harmonic values of current and voltage in AC system is balanced.
- The other harmonics except the main harmonic are ignored.
- The ripples in the form of DC current and voltages are ignored.
- The thyristors used in the converters are accepted as ideal switch and it is supposed to be short circuit in the direction of transmission and open circuit in the direction of plugging.
- No load current of the converter transformers and the losses are ignored.

An AC bus having generators, AC lines, shunt compensators and converters is represented in Fig. 1[30]. The active and reactive power equalities at such a bus are given by Eqs. (1) and (2).

$$p_{gk} = p_{lk} + p_{dk} + p_k \tag{1}$$

$$q_{gk} + q_{sk} = q_{lk} + q_{dk} + q_k \tag{2}$$

where p_{gk} is the active power generation of the kth bus; p_{lk} the active load of the kth bus; p_{dk} the active power transferred to dc line from the kth bus; p_k the active power transferred to ac line from the kth bus; q_{gk} the reactive power generation of the kth bus; q_{lk} the reactive load of the kth bus; q_{dk} the reactive power absorbed by the converter in the kth bus; q_k the reactive power transferred to ac line from the kth bus; q_{sk} the shunt compensator in the kth bus.

For rectifier bus,

$$p_{dk} = p_r \tag{3}$$

$$q_{dk} = q_r \tag{4}$$

For inverter bus,

$$p_{dk} = -p_i \tag{5}$$

$$q_{dk} = q_i \tag{6}$$

A basic schematic diagram of a two-terminal HVDC transmission link interconnecting buses "r" (rectifier) and "i" (inverter) is illustrated in Fig. 2. The basic converter equations describing the relationship between AC and DC variables were expressed in Ref. [31].

The variables shown in Fig. 2 are defined as follows:

v_r is the primary line-to-line ac voltage (rms) of the rectifier side.
V_i the primary line-to-line ac voltage (rms) of the inverter side.
φ_r the phase angle of the rectifier side.
φ_i the phase angle of the inverter side.
i_r ac current of the rectifier side.
i_i ac current of the inverter side.
v_{dr} the rectifier side voltage of DC link.
v_{di} the inverter side voltage of DC link.
i_d the direct current.
t the transformer tap ratio.

2.1. The equations for rectifier side of DC transmission link

The equations related to the rectifier operation of a converter can be expressed as follows:

$$v_{dor} = kt_r v_r \tag{7}$$

$$v_{dr} = v_{dor} \cos\alpha - r_{cr} i_d \tag{8}$$

where v_{dor} is the ideal no-load direct voltage, $k = 3\sqrt{2}/\pi$ and α is the ignition delay angle; r_{cr} the so called equivalent commutating resistance, which accounts for the voltage drop due to commutation overlap and is proportional to the commutation reactance, $r_{cr} = \sqrt{3}x_{cr}/\pi$. The active power for the rectifier side is determined by:

$$p_r = v_{dr} i_d \tag{9}$$

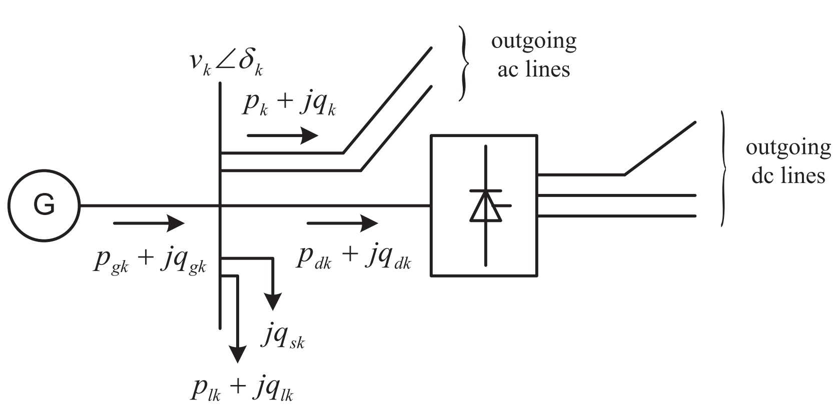

Fig. 1. The representation of the ac bus which is connected dc transmission link [30].

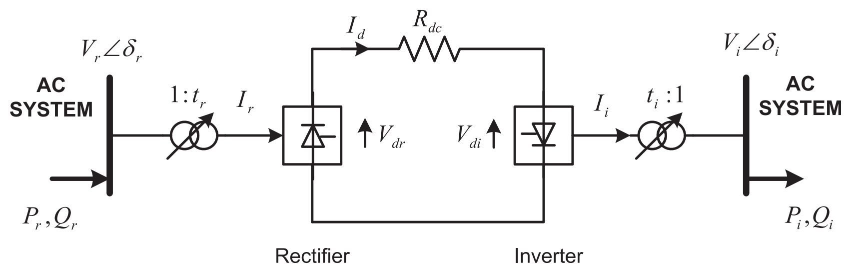

Fig. 2. A basic schematic diagram of a two-terminal HVDC transmission link [31].

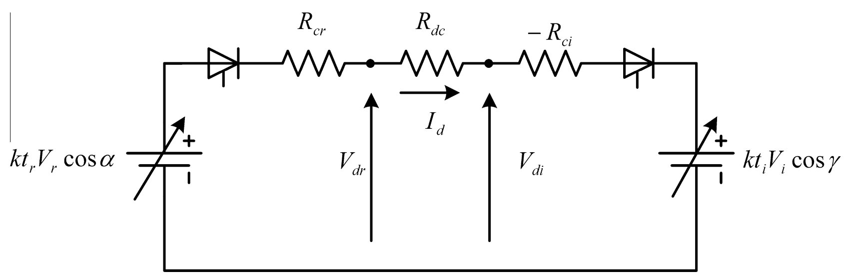

Fig. 3. The equivalent circuit of a two-terminal HVDC link [32].

Table 1
Cases with respect to the population sizes.

Cases	1	2	3	4	5
Initial population	10	20	30	40	50
Crossover	5	10	15	20	25
Mutation	1	2	3	4	5
Cases	6	7	8	9	10
Initial population	60	70	80	90	100
Crossover	30	35	40	45	50
Mutation	6	7	8	9	10

Since losses at the converter and transformer can be ignored ($p_r = p_{ac}$), the reactive power at the rectifier side is determined as follows:

$$q_r = |p_r tan\phi_r| \tag{10}$$

where ϕ_r is the phase angle between the AC voltage and the fundamental AC current and is calculated by neglecting the commutation overlap as follows:

$$\phi_r = \cos^{-1}(v_{dr}/v_{dor}) \tag{11}$$

The equivalent circuit of a two-terminal HVDC link is shown in Fig. 3[32] and the related relationships are given by Eqs. (8), (13), and (17).

2.2. The equations for inverter side of DC transmission link

The equations related to the inverter operation of a converter can be expressed as follows:

$$v_{doi} = kt_i v_i \tag{12}$$

$$v_{di} = v_{doi}\cos\gamma - r_{ci} i_d \tag{13}$$

$$p_i = v_{di} i_d \tag{14}$$

$$q_i = |p_i tan\phi_i| \tag{15}$$

$$\phi_i = \cos^{-1}(v_{di}/v_{doi}) \tag{16}$$

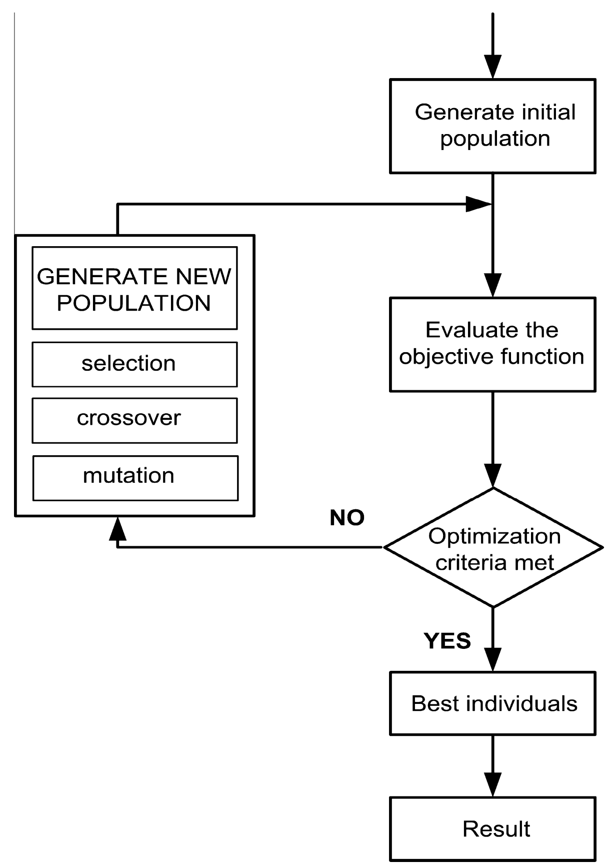

Fig. 4. The simple flow scheme of GA [35].

where γ is the extinction advance angle.

2.3. DC link equation

The relationship between the voltages of both sides of DC link voltages can be expressed by Eq. (17):

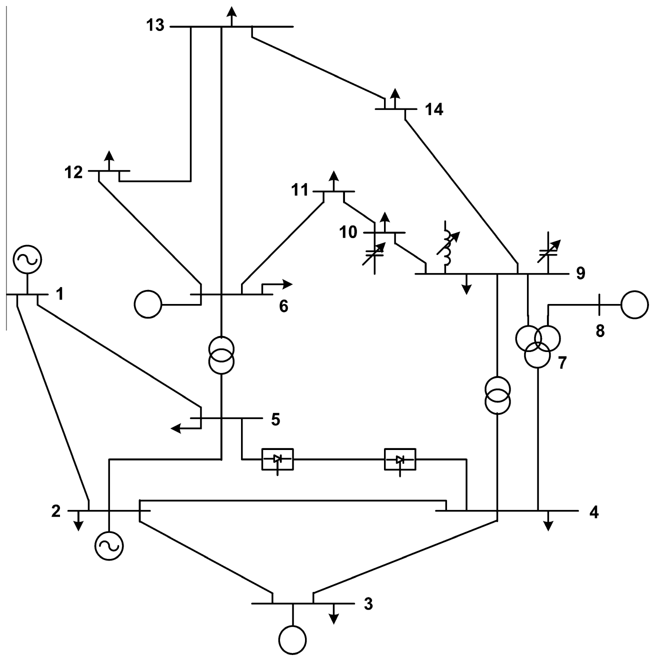

Fig. 5. The modified IEEE 14-bus test system [36].

Table 2
DC link characteristics for the modified 14-bus test system.

	Rectifier	Inverter
Bus number	5	4
Commutation reactance (p.u.)	0.1260	0.07275
DC link resistance (p.u.)	0.00334	

Table 3
Minimum, maximum, average fitness values and the computational times of the modified IEEE 14-bus test system using GA for all the cases.

Cases	Minimum fitness value	Maximum fitness value	Average fitness value	Time (s)
1	4.4413	50260.7	25132.57	13.66
2	3.8589	22681.4	11342.63	26.77
3	3.6099	4.4261	4.01800	37.43
4	3.6062	4.4092	4.00770	54.82
5	3.5476	4.1244	3.83600	67.65
6	3.5349	4.0601	3.79750	81.05
7	3.5045	4.0024	3.75345	94.72
8	3.4648	3.9056	3.68520	107.88
9	3.4631	3.8399	3.65150	121.54
10	3.4372	3.7769	3.60705	135.95

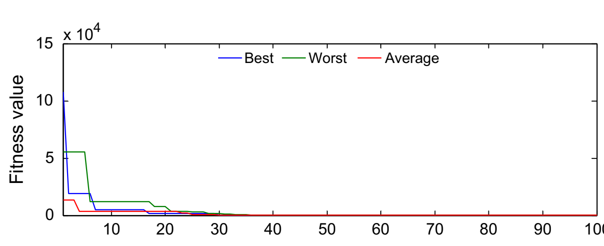

Fig. 6. The fitness values variations of the best, the worst and average individuals against iteration number of the modified IEEE 14-bus test system for the case 5.

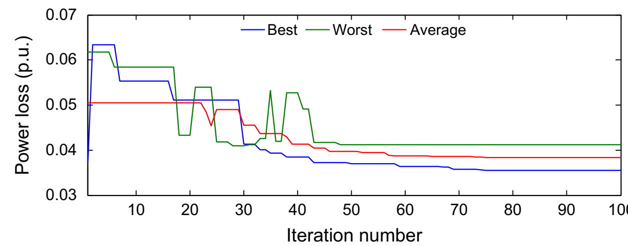

Fig. 7. The power loss variations of the best, the worst and average individuals against iteration number of the modified IEEE 14-bus test system for the case 5.

$$v_{dr} = v_{di} + r_{dc} i_d \quad (17)$$

where r_{dc} is DC link resistance.

3. Illustration of GA

GA is heuristic algorithm based on natural selection. GA's were firstly utilized by Holland in 1975 for solving optimization problems [33]. The base logic of the algorithm is that gens of powerful individuals are based to be carried over next generation and others are based to be detached in next generation. In natural selection, a human born, grows, and dies. These stages of human life correspond to the different operators in the algorithm. GA operators related these stages can be explained as the following.

3.1. Initial population

Initial population is determined in two ways. One of them is to form random individuals as initial population size within their limits. The second way is to form initial population of the certain individuals. The fitness values of individuals within population are obtained to be put in objective function the formed individuals. The individual number within initial population is randomly determined by Eq. (18).

$$w_{ij} = w_{\min,j} + rand(0,1) \times (w_{\max,j} - w_{\min,j}) \quad (18)$$

where the parameters $w_{\min,j}$ and $w_{\max,j}$ show the minimum and maximum of the variable w_j.

3.2. Fitness scaling

The scaling stage is one of GA operators. The scaling prevents algorithm to get stuck on a local point. There are different scaling methods as rank scales, top scales, and shift linear scales. In this study, the better individuals than individual having average fitness value are selected and can be formulated as follows:

Table 4
Comparative DC system results obtained by GA and Ref. [36] of the modified IEEE 14-bus test system for the case 5.

Variables	Limits		GA	Ref. [36]
	Low	High		
p_{dr}	0.10	1.50	0.6125	0.5000
p_{di}	0.10	1.50	0.6117	0.4995
q_{dr}	0.05	0.75	0.2067	0.1626
q_{di}	0.05	0.75	0.1950	0.1553
t_r	0.90	1.10	0.99	0.9722
t_i	0.90	1.10	0.98	0.9605
α (°)	7.00	15.00	14.5947	10.0216
γ (°)	10.00	20.00	14.9273	12.9585
v_{dr}	1.00	1.50	1.3080	1.3012
v_{di}	1.00	1.50	1.3064	1.3000
i_d	0.10	1.00	0.4683	0.3842

Table 5
Limits on the variables and comparative AC system results obtained by GA and Ref. [36] of the modified IEEE 14-bus test system for the case 5.

Variables (p.u.)	Limits		Results	
	Low	High	GA	Ref. [36]
p_{g1}	0.0000	3.3240	0.5458	–
p_{g2}	0.0000	2.0000	1.0803	–
q_{g1}	−0.1000	0.5000	0.0003	−0.0838
q_{g2}	−0.1000	0.5000	0.0548	−0.0981
q_{c3}	−0.1000	1.0000	0.17	0.2873
q_{c6}	−0.1000	1.0000	0.51	0.1815
q_{c8}	−0.1000	0.8000	0.09	0.327
q_{c9}	0.0000	0.2000	0.18	0.00
q_{c10}	0.0000	0.2000	0.10	0.00
v_1	1.0000	1.1500	1.060	1.0707
v_2	1.0000	1.1500	1.056	1.0618
v_3	1.0000	1.1500	1.041	1.0747
v_4	0.9500	1.0500	1.036	1.0495
v_5	0.9500	1.0500	1.036	1.0422
v_6	1.0000	1.1500	1.041	1.0620
v_7	0.9500	1.0500	1.030	1.0498
v_8	1.0000	1.1500	1.045	1.1021
v_9	0.9500	1.0500	1.045	1.0499
v_{10}	0.9500	1.0500	1.044	1.0447
v_{11}	0.9500	1.0500	1.040	1.0500
v_{12}	0.9500	1.0500	1.027	1.0470
v_{13}	0.9500	1.0500	1.024	1.0427
v_{14}	0.9500	1.0500	1.018	1.0286
$t(5–6)$	0.9000	1.1000	1.07	1.0015
$t(4–7)$	0.9000	1.1000	1.05	1.0546
$t(4–9)$	0.9000	1.1000	0.93	0.9162
Power loss (p.u.)			0.035476	0.0425

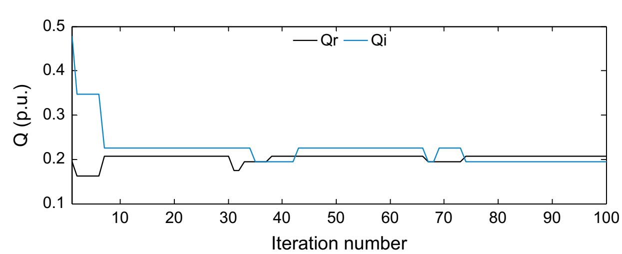

Fig. 8. The reactive power variations at rectifier and inverter sides against iteration number for the modified IEEE 14-bus test system.

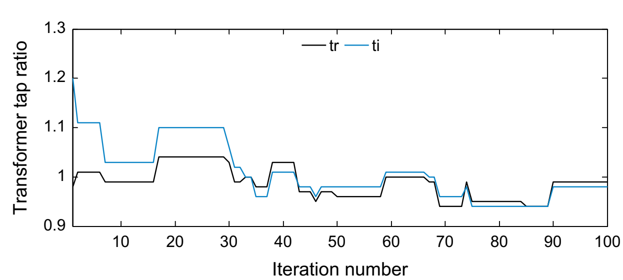

Fig. 9. Transformer tap ratio variations at rectifier and inverter sides against iteration number for the modified IEEE 14-bus test system.

$$F_{ave} = \frac{\sum_{i=1}^{N_k} F_i}{N_k} \tag{19}$$

where F_{ave}, N_k, and F_i represent the average fitness value within population, the number of individuals within population, and the fitness value of ith individual, respectively.

3.3. Selection

In this stage, the parents to be crossed for producing a child are selected. There are different selection methods as stochastic uniform, remainder, uniform, shift linear, roulette and tournament. In this study, the tournament method is preferred and can be formulated as follows:

$$\tau_i = \frac{F_i}{\sum_{j=1}^{N_k} F_j} \tag{20}$$

where τ_i represents the weight of ith individual within population. Furthermore, the sum of the elective probabilities of all the individuals within population is 1 as given by Eq. (21).

$$\sum_{i=1}^{N_k} \tau_i = 1 \tag{21}$$

The twice individual of the children number determined in the beginning of the algorithm is selected from individuals within population for crossover. The percentage distribution of the individuals within population is proportional to its fitness value. The best individuals are shown by the high-level percentage distributions in roulette selection. After all the individuals are shown as the percentage distribution between 0 and 1, the roulette selection in the definite number is performed. Thus, the individuals are selected for crossover.

3.4. Crossover

In this stage, a child is produced to be crossed the parents. New individuals same as the determined number are produced to be used the crossing method with the scattered parameter from parents selected via the tournament method explained in selection stage.

The value of 1 and 0 as gen number of an individual is randomly produced. If the value is 1, then gen is taken from mother, the value is 0, then gen is taken from father and thus the child is produced.

Cross: 1 0 1 1 0
Mother: a b c d e
Father: x y z u w
Child: a y c d w

3.5. Mutation

In mutation stage, new individuals are produced to be changed all or some gens of the selected individuals within population. The number of individual undergo mutation has to be determined in the beginning of the algorithm. The individuals undergo mutation are reproduced to be formed all the gens of the selected individuals within algorithm. Thus, new individuals as the number determined by Eq. (18) are randomly produced.

3.6. The stopping criterion of algorithm

There are many criterions for stopping algorithm. Some of these are the fitness value, time, and iteration number. In this study, iteration number is preferred as the stopping criterion. More information related to GA operators is available in Ref. [34]. Final population is formed to be included the reproduced individuals in stages above to initial population. After the individuals within final population are classified according to fitness value, the individual same as initial population is carried over the next iteration. A simple flow scheme of GA is shown in Fig. 4 [35].

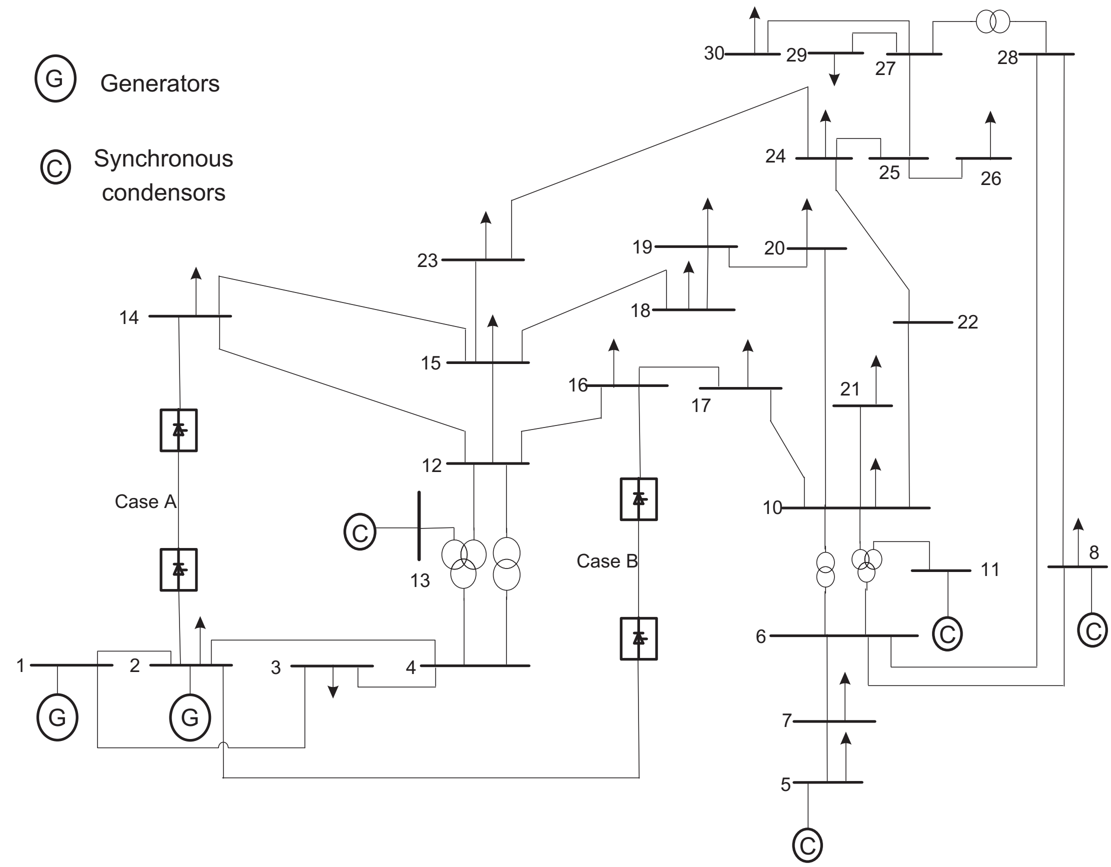

Fig. 10. The modified IEEE 30-bus system [37].

Table 6
Minimum, maximum and average fitness values and the computational times of the modified IEEE 30-bus test system using GA for all the cases.

Cases	Case A		Case B		Time (s)
	Min.	Max.	Min.	Max.	
1	13.1991	9638.4	13.8739	98282	14.89
2	12.7144	8267.8	13.8671	48105	29.82
3	12.5840	1016.29	12.2364	34138	46.23
4	12.4832	197.680	12.1307	11216	62.40
5	12.4065	14.2020	12.0150	13.5989	74.86
6	12.1908	13.4281	11.6110	12.2419	89.47
7	12.1855	13.0647	11.5668	12.1656	107.84
8	11.9083	12.7198	11.5198	12.1189	119.85
9	11.7488	12.5078	11.4933	12.0325	134.50
10	11.7081	12.1332	11.4872	11.8849	153.78

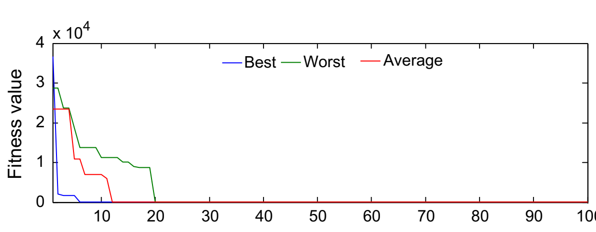

Fig. 11. For Case A, the fitness value variations of the best, the worst and average individuals against iteration number of the modified IEEE 30-bus test system for the case 5.

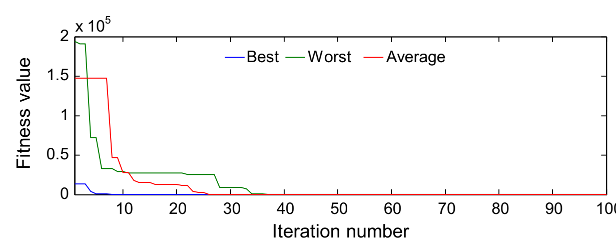

Fig. 12. For Case B, the fitness value variations of the best, the worst and average individuals against iteration number of the modified IEEE 30-bus test system for the case 5.

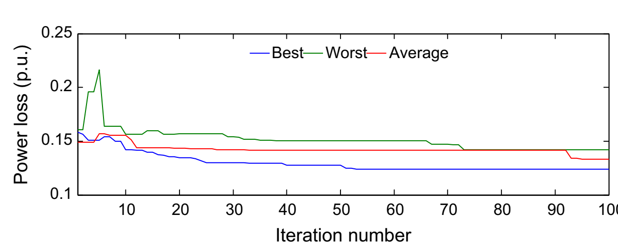

Fig. 13. For Case A, the power loss variations of the best, the worst and average individuals against iteration number of the modified IEEE 30-bus test system for the case 5.

4. Optimizing reactive power flow of HVDC systems using GA

In order to solve ORPF problem of HVDC systems, we have to determine the control and the variables. The control variables

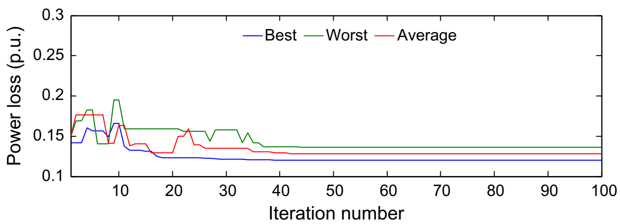

Fig. 14. For Case B, the power loss variations of the best, the worst and average individuals against iteration number of the modified IEEE 30-bus test system for the case 5.

Table 7
Comparative DC system results obtained by GA and Ref. [37].

Variables	Limits		Case A		Case B	
	Low	High	GA	Ref. [37]	GA	Ref. [37]
p_{dr}	0.10	1.50	0.2749	0.2502	0.2749	0.2503
p_{di}	0.10	1.50	0.2719	–	0.2720	–
q_{dr}	0.05	0.75	0.0641	0.1000	0.0752	0.1002
q_{di}	0.05	0.75	0.0664	–	0.0614	–
t_r	1.00	1.10	1.00	1.0020	1.02	1.025
t_i	1.00	1.10	1.00	1.0034	1.00	1.020
α (°)	9.74	22.91	12.5255	22.5630	14.9068	22.9125
γ (°)	8.59	22.91	13.8534	14.6276	12.1654	22.6833
v_{dr}	1.00	1.50	1.3786	–	1.3800	–
v_{di}	1.00	1.50	1.3636	–	1.3651	–
i_d	0.10	1.00	0.1994	0.1007	0.1992	0.3000

should be the same as those of the problem to be optimized. The control variables of the AC–DC system are:

$$u = [u_{AC}, u_{DC}] \tag{22}$$

$$u_{AC} = [p_{g2}, \ldots, p_{gNg}, v_{g1}, \ldots, v_{gNg}, q_{s1}, \ldots, q_{sN_s}, t_1, \ldots, t_{N_T}]. \tag{23}$$

$$u_{DC} = [p_r, p_i, q_r, q_i, i_d] \tag{24}$$

where p_{gi} except the slack unit p_{slack} is the generator active power outputs, v_{gi} the generator voltage, N_g the number of generator buses, N_s the number of shunt compensators and N_T the number of transformers, respectively.

The state variables of the AC–DC system are:

$$x = [x_{AC}, x_{DC}] \tag{25}$$

$$x_{AC} = [p_{gslack}, q_{g1}, \ldots, q_{gNg}, v_{l1}, \ldots, v_{lN_l}] \tag{26}$$

$$x_{DC} = [t_r, t_i, \alpha, \gamma, v_{dr}, v_{di}] \tag{27}$$

where p_{gslack} is the slack bus active power output, q_{gi} the reactive power output, v_{li} the load bus voltage, N_l the number of load buses, respectively.

For updating active and reactive power at rectifier and inverter bus, we use the following formulas:

For rectifier bus:

$$\begin{aligned} p_{load}^{update} &= p_{load} + p_r \\ q_{load}^{update} &= q_{load} + q_r \end{aligned} \tag{28}$$

For inverter bus:

$$\begin{aligned} p_{load}^{update} &= p_{load} - p_i \\ q_{load}^{update} &= q_{load} + q_i \end{aligned} \tag{29}$$

The fitness value for each individual is obtained by Eq. (30) as follows:

Table 8
Limits on the variables and comparative AC system results obtained by GA and Ref. [37] of the modified IEEE 30-bus test system for the case 5.

Variables (p.u.)	Limits		Case A		Case B	
	Low	High	GA	Ref. [37]	GA	Ref. [37]
p_{g1}	0.00	3.602	1.6057	–	1.5897	–
p_{g2}	0.00	1.40	1.3552	–	1.3673	–
q_{g1}	−1.00	1.00	0.2951	−0.7280	0.1921	0.4065
q_{g2}	−0.40	0.50	0.2605	0.4890	0.2027	0.3101
q_{c5}	−0.40	0.40	0.34	0.3882	0.39	0.0362
q_{c8}	−0.10	0.40	0.32	0.3988	0.32	0.3343
q_{c11}	−0.06	0.24	0.08	0.2351	0.19	0.2311
q_{c13}	−0.06	0.24	0.23	0.1438	0.23	0.0865
v_1	1.00	1.15	1.075	1.1114	1.063	1.0994
v_2	1.00	1.15	1.050	1.0883	1.041	1.0867
v_3	0.90	1.05	1.026	–	1.021	–
v_4	0.90	1.05	1.014	–	1.010	–
v_5	1.00	1.15	1.007	1.0708	1.006	1.0754
v_6	0.90	1.05	1.003	–	1.002	–
v_7	0.90	1.05	0.997	–	0.996	–
v_8	1.00	1.15	1.001	1.0585	1.000	1.0679
v_9	0.90	1.05	1.049	–	1.047	–
v_{10}	0.90	1.05	1.019	–	1.031	–
v_{11}	1.00	1.15	1.064	1.1159	1.084	1.1064
v_{12}	0.90	1.05	1.047	–	1.049	–
v_{13}	1.00	1.15	1.077	1.0555	1.079	1.0211
v_{14}	0.90	1.05	1.044	–	1.033	–
v_{15}	0.90	1.05	1.024	–	1.028	–
v_{16}	0.90	1.05	1.027	–	1.038	–
v_{17}	0.90	1.05	1.017	–	1.028	–
v_{18}	0.90	1.05	1.010	–	1.017	–
v_{19}	0.90	1.05	1.004	–	1.013	–
v_{20}	0.90	1.05	1.007	–	1.017	–
v_{21}	0.90	1.05	1.007	–	1.018	–
v_{22}	0.90	1.05	1.008	–	1.019	–
v_{23}	0.90	1.05	1.010	–	1.016	–
v_{24}	0.90	1.05	1.000	–	1.009	–
v_{25}	0.90	1.05	1.010	1.0049	1.020	0.9935
v_{26}	0.90	1.05	0.992	0.9823	1.002	0.9716
v_{27}	0.90	1.05	1.025	1.0129	1.035	0.9940
v_{28}	0.90	1.05	0.997	–	0.996	–
v_{29}	0.90	1.05	1.005	0.9676	1.015	0.9502
v_{30}	0.90	1.05	0.994	0.9714	1.004	0.9547
t(6–9)	0.90	1.10	0.92	1.0269	0.96	1.0001
t(6–10)	0.90	1.10	1.01	1.0000	0.93	1.0000
t(4–12)	0.90	1.10	0.95	1.0000	0.95	1.0001
t(28–27)	0.90	1.10	0.94	1.0010	0.93	1.0380
Power loss (p.u.)			0.1240	0.2841	0.1201	0.2811

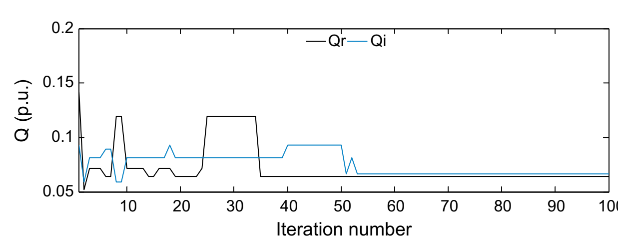

Fig. 15. For Case A, the reactive power variations at rectifier and inverter sides against iteration number for the modified IEEE 30-bus test system.

$$\begin{aligned} F_i = {} & K_1 p_{Loss} + K_2|p_{slack} - p_{slack}^{\lim}| + K_3\sum_{i=1}^{N_g}|q_{gi} - q_{gi}^{\lim}| + K_4\sum_{i=1}^{N_l}|v_{li} \\ & - v_{li}^{\lim}| + K_5|t_r - t_r^{\lim}| + K_6|t_i - t_i^{\lim}| + K_7|\alpha - \alpha^{\lim}| + K_8|\gamma \\ & - \gamma^{\lim}| + K_9|v_{dr} - v_{dr}^{\lim}| + K_{10}|v_{di} - v_{di}^{\lim}| \end{aligned} \tag{30}$$

where $p_{slack}^{\lim}$, $q_{gi}^{\lim}$, $v_{li}^{\lim}$, $t_r^{\lim}$, $t_i^{\lim}$, $\alpha^{\lim}$, $\gamma^{\lim}$, $v_{dr}^{\lim}$ and $v_{di}^{\lim}$ show the limits of the related variables, respectively; $K_1, K_2, K_3, K_4, K_5, K_6, K_7, K_8, K_9,$ and K_{10} are penalty weights of power loss, real power output of

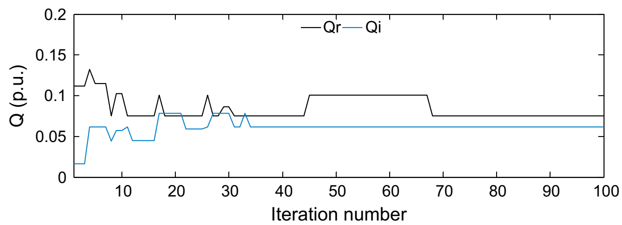

Fig. 16. For Case B, the reactive power variations at rectifier and inverter sides against iteration number for the modified IEEE 30-bus test system.

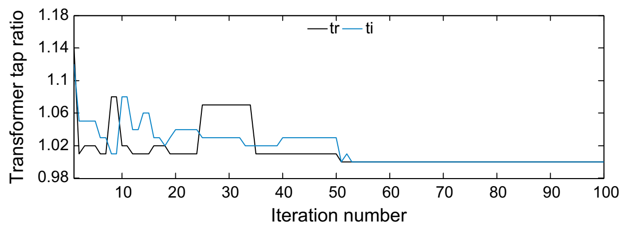

Fig. 17. For Case A, transformer tap ratio variations at rectifier and inverter sides against iteration number for the modified IEEE 30-bus test system.

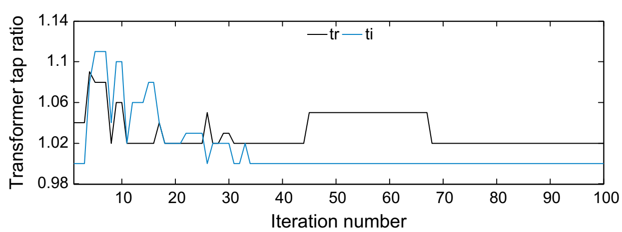

Fig. 18. For Case B, transformer tap ratio variations at rectifier and inverter sides against iteration number for the modified IEEE 30-bus test system.

slack bus, reactive power outputs of generator buses, load bus voltage magnitudes, the effective transformer ratio's of rectifier and inverter sides, the angles of rectifier and inverter sides, the direct voltages of rectifier and inverter sides respectively. Note that the value of penalty function grows with a quadratic form when the constraints are violated and is 0 in the region where constraints are not violated.

The power flow calculation for each individual in heuristic methods is performed and a fitness value F_i for each individual is calculated to evaluate its quality as follows:

Step 1: Update p_{load} and q_{load} at rectifier and inverter sides by using Eqs. (28) and (29)
Step 2: Run Newton-Raphson
Step 3: Calculate the values of t_r, t_i, α, γ, v_{dr}, v_{di}
Step 4: Calculate the fitness value F_i by using Eq. (30)

$$p_{loss} = \sum_{i=1}^{N_g} p_{gi} - \sum_{j=1}^{N} p_{lj} \tag{31}$$

where p_{loss} represents the real power transmission line losses, p_{lj} represents the active load of jth bus.

The flowchart of genetic algorithm is defined as follows:

Step 1. Read system data and GA parameters.
Step 2. Generate initial population of n individuals via control variable u.
Step 3. Calculate the fitness value F_i of each chromosome in the population.
Step 4. Create a new population by repeating the following steps until the new population is completed.
Step 5. Select the parents by tournament selection.
Step 6. Crossover the parent chromosomes to form a new child with scattered.
Step 7. Mutate new child with a mutation probability.
Step 8. Calculate the fitness F_i of each new child.
Step 9. Include new child to the population.
Step 10. Classify the all individuals from minimum to maximum.
Step 11. Carry over the individual same as initial population to the next iteration.
Step 12. If the stopping criterion is satisfied, stop algorithm and show the best solution in current population else, go to Step 4..

5. Application of GA on test systems and the simulation results

In this study, the proposed method is applied to four different test systems those are the modified IEEE 14-bus test system, the modified IEEE 30-bus test system and the modified New England 39-bus test system. The simulations are performed for different population sizes given in Table 1. For these systems, minimum, maximum, average fitness values and the computational times obtained by GA are given in the bottom. It can be seen from results that the optimum solution is not obtained by increasing the population size and the computational times of the software increase as the population size increases. The optimum solution is obtained by trials. The crossover rate and the mutation rate inside of the algorithm are taken into account as a constant such as the population can be compared to other studies. These values are 50% and 10%, respectively. Furthermore, the results obtained by the proposed method are compared to those reported in literature. The proposed algorithm is run on a computer with I3 CPU 2.4 GHz, 2 GB RAM. In order to test the validity, the effectiveness, and the efficiency of the proposed method, the test systems mentioned above are used. The algorithm proposed in this study is developed via real GA codes without using GA tool on Matlab.

In this study, the transformer tap ratios and the switchable shunt capacitor/reactor banks are taken into consideration as discrete variables. The transformer tap-step and the bank/unit capacity-step are also selected as being 0.01 p.u.

5.1. The modified IEEE 14-bus test system

The modified IEEE 14-bus test system is shown in Fig. 5[36]. A two-terminal HVDC link is included to between buses 4 and 5 in the original IEEE 14-bus test system. This system has 20 ac transmission lines, 2 generators, 3 transformers, 3 synchronous condensers and 2 switchable VAR compensators. The bus 4 is selected as rectifier and then the bus 5 is selected as inverter bus.

The characteristics of DC transmission link are given in Table 2.

For all the cases, minimum, maximum, average fitness values and the computational times obtained by GA for the modified IEEE 14-bus test system are given Table 3. Although the computational times of the software are very low for the population sizes in cases 1, and 2 minimum, maximum and average fitness values are so much and the variables exceed their limits. The variables do not exceed their limits for the population sizes in cases 3–10. For these cases, it can be seen from Table 3 that the computational times increase considerably, as the average fitness values decrease from case 3 to case 10. In order to show the superiority of the proposed method, the population size which obtains better than solution reported in literature is determined as best one. Therefore optimum population size for this test system is taken into account as case 5.

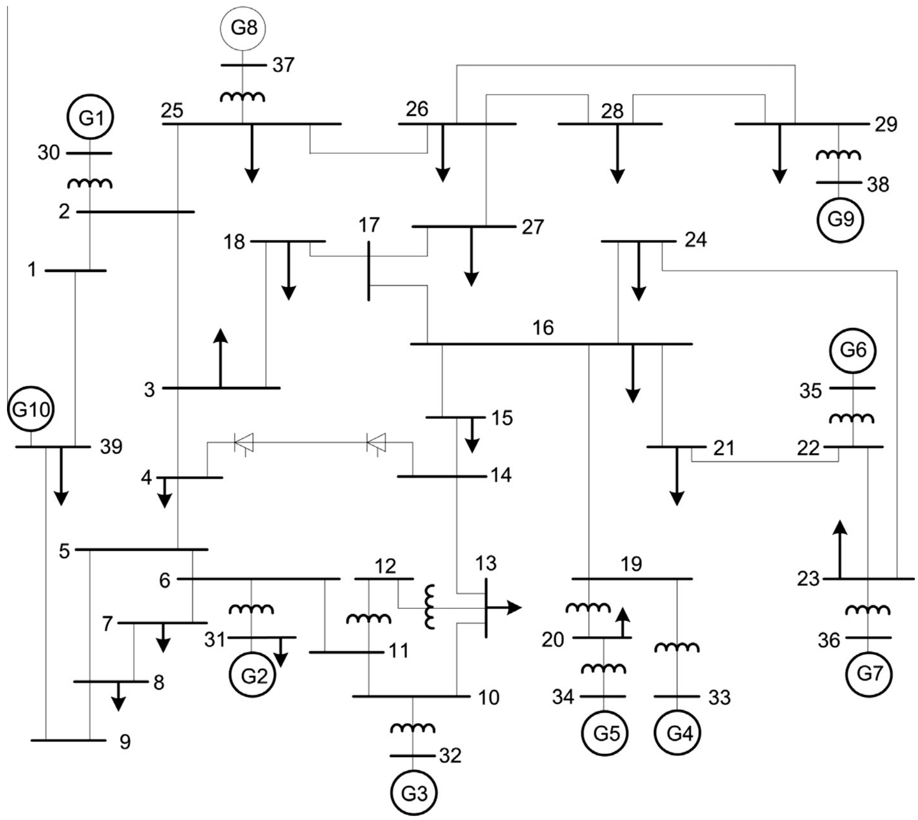

Fig. 19. The modified New England 39-bus system [38].

Table 9
Minimum, maximum, average fitness values and the computational times of the modified New England 39-bus test system using GA for all the cases.

Cases	Minimum fitness value	Maximum fitness value	Average fitness value	Time (s)
1	44.5042	513933.5	256989	25.3
2	40.8734	196732	98386.44	51.1
3	39.546	4665.05	2352.298	72.3
4	38.4446	1806.05	922.2473	99.6
5	37.1844	56.4434	46.8139	121.4
6	36.1538	47.4554	41.8046	150.6
7	35.5116	46.1185	40.81505	178.9
8	35.4762	45.0288	40.2525	209.6
9	35.0795	43.6327	39.3561	229.8
10	34.8669	42.5273	38.6971	250.4

For the case 5, the fitness values variations of the best, the worst and average individuals against iteration number of the modified IEEE 14-bus test system are shown in Fig. 6.

The power loss variations of the best, the worst and average individuals against iteration number of the modified IEEE 14-bus test system for the case 5 are shown in Fig. 7.

For the case 5, comparative DC system results obtained by GA and Ref. [36] of the modified IEEE 14-bus test system are given in Table 4.

Comparative AC system results obtained by GA and Ref. [36] of the modified IEEE 14-bus test system for the case 5 are given in Table 5. As can be evidently seen from Table 5, the power loss obtained by GA is lesser than that reported in Ref. [36] by 16.32%.

The reactive power variations at rectifier and inverter sides against iteration number for the modified IEEE 14-bus test system are shown in Fig. 8.

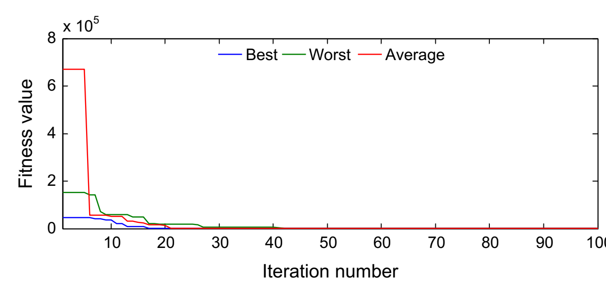

Fig. 20. The fitness values variations of the best, the worst and average individuals against iteration number of the modified New England 39-bus test system for the case 5.

Transformer tap ratio variations at rectifier and inverter sides against iteration number for the modified IEEE 14-bus test system are shown in Fig. 9.

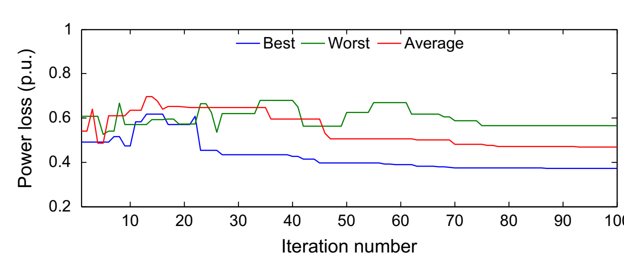

Fig. 21. The power loss variations of the best, the worst and average individuals against iteration number of the modified New England 39-bus test system for the case 5.

Table 10
DC system results for the modified New England 39-bus test system.

		Control angles (°)	Tap-ratio	Active power (p.u.)	Reactive power (p.u.)	DC current (p.u.)
GA	Rec.	9.364390	0.93	0.910674	0.317602	0.757387
	Inv.	10.979469	0.94	0.908758	0.286124	

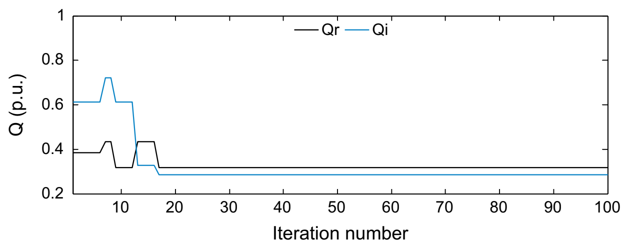

Fig. 22. The reactive power variations at rectifier and inverter sides against iteration number for the modified New England 39-bus test system.

5.2. The modified IEEE 30-bus test system

The data of the modified IEEE 30-bus test system is given in Ref. [37]. The study is realized for different cases of the modified IEEE 30-bus test system. These are;

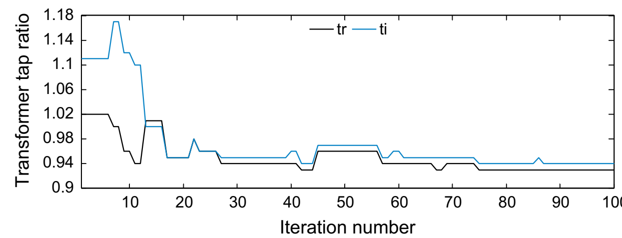

Fig. 23. Transformer tap ratio variations at rectifier and inverter sides against iteration number for the modified New England 39-bus test system.

HVDC Case A: A two-terminal HVDC link is included to between buses 2 (rectifier bus) and 14 (inverter bus) in the original IEEE 30-bus test system.

HVDC Case B: A two-terminal HVDC link is included to between buses 2 (rectifier bus) and 16 (inverter bus) in the original IEEE 30-bus test system.

For both HVDC cases, the modified IEEE 30-bus test system is shown in Fig. 10.

For both HVDC cases, the maximum, minimum and average fitness values and the computational times obtained for different population sizes are given in Table 6.

As can be evidently seen from Table 6, for some trials in the population cases of 1–4, the minimum fitness values are within the normal range whereas the maximum fitness values exceed the normal range.

Table 11
AC system results for the modified New England 39-bus test system.

Bus number	v (p.u.)	Angle (°)	p_g (p.u.)	q_g (p.u.)	Transformer tap ratio	
1	1.000	−10.043	–	–	t_{12-11}	1.03
2	1.022	−8.1610	–	–	t_{12-13}	1.05
3	1.014	−11.703	–	–	t_{6-31}	1.04
4	0.987	−12.588	–	–	t_{10-32}	0.96
5	0.999	−10.166	–	–	t_{19-33}	1.06
6	1.003	−9.270	–	–	t_{20-34}	0.95
7	0.991	−11.463	–	–	t_{22-35}	0.98
8	0.990	−11.957	–	–	t_{23-36}	1.02
9	1.008	−10.824	–	–	t_{25-37}	1.00
10	1.018	−6.395	–	–	t_{2-30}	0.99
11	1.012	−7.368	–	–	t_{29-38}	1.00
12	1.024	−7.284	–	–	t_{19-20}	1.03
13	1.015	−7.071	–	–		
14	1.013	−8.619	–	–		
15	1.006	−10.84	–	–		
16	1.015	−10.161	–	–		
17	1.024	−11.302	–	–		
18	1.019	−11.896	–	–		
19	1.013	−5.601	–	–		
20	1.007	−6.683	–	–		
21	1.005	−8.032	–	–		
22	1.009	−3.671	–	–		
23	1.012	−4.078	–	–		
24	1.020	−10.172	–	–		
25	1.036	−7.359	–	–		
26	1.057	−10.783	–	–		
27	1.038	−12.186	–	–		
28	1.051	−9.64	–	–		
29	1.040	−7.576	–	–		
30	1.016	−4.88	3.28362	−0.26788		
31	1.000	0.00	6.24765	2.366		
32	1.014	1.747	7.02286	2.28483		
33	1.059	−1.524	5.60843	0.20751		
34	0.973	−0.699	5.41427	1.24117		
35	1.059	0.893	6.25942	−0.037		
36	1.050	2.904	4.86081	0.90016		
37	1.009	0.541	6.07412	−0.02089		
38	1.024	−2.228	6.34158	−1.7428		
39	0.963	−9.777	11.80329	−2.43789		
Power loss (p.u.)			0.37184	–		

The minimum and maximum fitness values are within the normal range in the population cases of 5–10. Although the computational time difference between population cases 5 and 10 is great, the fitness value difference between cases 5 and 10 is low. On this account, acceptable population size is determined as case 5 for both HVDC cases.

For both HVDC cases, the fitness value variations of the best, the worst and average individuals against iteration number are shown in Figs. 11 and 12, respectively.

For both HVDC cases, power loss variations of the best, the worst and average individuals against iteration number are shown in Figs. 13 and 14, respectively.

Comparative DC system results obtained by GA and Ref. [37] are given in Table 7.

Comparative AC system results obtained by GA and Ref. [37] are given in Table 8. As can be evidently seen from Table 8, the power losses obtained by GA and the numerical method in Ref. [37] for HVDC Case A are 0.1240 and 0.2841, respectively. The power losses obtained by GA and the numerical method in Ref. [37] for HVDC Case B are also 0.1201 and 0.2811, respectively. For both HVDC cases, the results obtained by GA are lesser than those reported in Ref. [37] by 56.35% and 57.27%, respectively.

For both HVDC cases, the reactive power variations at rectifier and inverter sides against iteration number are shown in Figs. 15 and 16, respectively.

For both HVDC cases, transformer tap ratio variations at rectifier and inverter sides against iteration number are shown in Figs. 17 and 18, respectively.

For both HVDC cases, as can be evidently seen from Figs. 17 and 18 that the transformer tap ratios are within limits at the end of the iteration.

5.3. The modified New England 39-bus test system

AC transmission line between buses 4 and 14 in the original New England 39-bus test system is replaced with a two terminal HVDC link and the modified New England 39-bus test system shown in Fig. 19 is obtained [38]. The upper and lower limits of the transformer tap ratios in power system are 1.1 p.u. and 0.9 p.u., respectively. DC link data for this test system is the same as that of the modified 14 bus-test system.

The simulation results obtained by the trials are given in Table 9.

By reason of comparison of the fitness values and the computational times, the optimum solution is determined as case 5. For case 5, the variations of the best, the worst, and the average fitness values against iteration number is shown in Fig. 20.

The power loss variations of the best, the worst and average individuals against iteration number for case 5 of the modified New England 39-bus test system are shown in Fig. 21.

AC and DC system variables obtained by the proposed algorithm are given in Tables 10 and 11, respectively.

The reactive power variations at rectifier and inverter sides against iteration number for the modified New England 39-bus test system are shown in Fig. 22.

Transformer tap ratio variations at rectifier and inverter sides against iteration number for the modified New England 39-bus test system are shown in Fig. 23.

6. Conclusion and discussion

In this study, ORPF problem of an integrated AC–DC power system is firstly solved by GA. In order to show the validity, the efficiency, and the effectiveness of GA, ORPF problem of an integrated AC–DC power system is tested on three test systems which are the modified IEEE 14-bus test system, the modified IEEE 30-bus test system and the modified New England 39-bus test system. As can be evidently seen from Tables 5 and 8, ORPF results obtained by GA for the modified IEEE 14-bus test system and the modified IEEE 30-bus test system is lesser than those obtained by the numerical method in Ref. [36,37]. As can be evidently seen GA is also faster than the numerical methods in terms of the convergence times. In comparison with other methods, GA converges reliably and rapidly to the true optimal point. In future, this algorithm and the other heuristic algorithms can be applied to ORPF of the large-scale multi-terminal HVDC systems.

As a result, it can be seen that the size of the system is not proportional to the population size and it is needed to make trials with respect to different population sizes for each system.

References

[1] Wu Y-C, Debs AS, Marsten RE. A nonlinear programming approach based on an interior point method for optimal power flows. Athens Power Technol 1993:196–200.
[2] Grudinin N. Reactive power optimization using successive quadratic programming method. IEEE Trans Power Syst 1998;13(4):1219–25.
[3] Mangoli MK, Lee KY, Park YM. Optimal real and reactive power control using linear programming. Electric Power Syst Res 1993;26(1):1–10.
[4] Gomes JR, Saavedra OR. Optimal reactive power dispatch using evolutionary computation: extended algorithms. IEE Proc-Gen Transmiss Distrib 1991;146(6):586–92.
[5] Iba K. Reactive power optimization by genetic algorithm. IEEE Trans Power Syst 1994;9(2):685–92.
[6] Wu QH, Cao YJ, Wen JY. Optimal reactive power dispatch using an adaptive genetic algorithm. Int J Electr Power Energy Syst 1998;20(8):563–9.
[7] Liu Y, Ma L, Zhang J. Reactive power optimization by GA/SA/TS combined algorithms. Int J Electr Power Energy Syst 2002;24(9):765–9.
[8] Li Y, Wang Y, Li B. A hybrid artificial bee colony assisted differential evolution algorithm for optimal reactive power flow. Int J Electr Power Energy Syst 2013;52:25–33.
[9] Çobanlı S, Öztürk A, Güvenç U, Tosun S. Active power loss minimization in electric power systems through artificial bee colony algorithm. Int Rev Electr Eng 2010;5(5):2217–23.
[10] Yan W, Lu S, Yu DC. A novel optimal reactive power dispatch method based on an improved hybrid evolutionary programming technique. IEEE Trans Power Syst 2004;19(2):913–8.
[11] Yoshida H, Kawata K, Fukuyama Y, Takayama S, Nakanishi Y. A particle swarm optimization for reactive power and voltage control considering voltage security assessment. IEEE Trans Power Syst 2000;15(4):1232–9.
[12] Ayan K, Kılıç U. Artificial bee colony algorithm solution for optimal reactive power flow. Appl Soft Comput 2012;12(5):1477–82.
[13] Varadarajan M, Swarup KS. Differential evolutionary algorithm for optimal reactive power dispatch. Int J Electr Power Energy Syst 2008;30(8):411–35.
[14] Latorre HF, Ghandhari M. Improvement of power system stability by using a VSC-HVDC. Int J Electr Power Energy Syst 2011;33(2):332–9.
[15] Sato H, Arrillaga J. Improved load-flow techniques for integrated AC–DC systems. Proc IEE 1969;116(4):525–32.
[16] Arifoğlu U. The power flow algorithm for balanced and unbalanced bipolar multiterminal ac/dc systems. Electr Power Syst Res 2003;64(3):239–46.
[17] Arifoğlu U. Load flow based on newton's method using norton equivalent circuit for an AC–DC multiterminal system. Eur Trans Electr Power (ETEP) 1999;9(3):167–74.
[18] Ambriz-Pérez H, Acha E, Fuerte-Esquivel CR. High voltage direct current modeling in optimal power flows. Int J Electr Power Energy Syst 2008;30(3):157–68.
[19] Fudeh H, Ong CM. A simple and efficient AC–DC load-flow method for multiterminal DC systems. IEEE Trans Power Apparat Syst 1981;PAS-100(11):4389–96.
[20] Kimbark E. Direct current transmission. New-York: Wiley-Interscience; 1971.
[21] Reeve J, Fahny G, Stott B. Versatile load flow method for multiterminal HVDC systems. IEEE Trans Power Apparat Syst 1977;96(3):925–33.
[22] Arrillaga J, Arnold CP, Harker BJ. Computer modeling of electric power systems. John Wiley and Sons; 1983.
[23] Smed T, Andersson G, Sheble GB, Gigsby LL. A new approach to AC–DC power flow. IEEE Trans Power Syst 1991;6(3):1238–44.
[24] Subbaraj P, Rajnarayanan PN. Optimal reactive power dispatch using self-adaptive real coded genetic algorithm. Electr Power Syst Res 2009;79(2):374–81.
[25] Szuvovivski I, Fernandes TSP, Aoki AR. Simultaneous allocation of capacitors and voltage regulators at distribution networks using Genetic Algorithms and Optimal Power Flow. IntJ Electr Power Energy Syst 2012;40(1):62–9.
[26] Wirmond VE, Fernandes TSP, Tortelli OL. TCPST allocation using optimal power flow and Genetic Algorithms. Int J Electr Power Energy Syst 2011;33(4):880–6.
[27] Walters DC, Sheble GB. Genetic algorithm solution for economic dispatch with valve point loading. IEEE Trans Power Syst 1993;8(3):1325–32.

[28] Goldberg DE. Genetic algorithms in search, optimization and machine learning. Addison Wesley Publishing Company; 1989.
[29] Kumari MS, Maheswarapu S. Enhanced genetic algorithm based computation technique for multi-objective optimal power flow solution. Int J Electr Power Energy Syst 2010;32(6):736–42.
[30] Lu CN, Chen SS, Ong CM. The incorporation of HVDC equations in optimal power flow methods using sequential quadratic programming techniques. IEEE Trans Power Syst 1988;3(3):1005–11.
[31] Mustafa MW, Abdul Kadir AF. A modified approach for load flow analysis of integrated AC–DC power systems. In: TENCON 2000. Proceedings, vol. 2; 2000. p. 108–13.
[32] Kundur P. Power system stability and control. New York: McGraw Hill; 1994.
[33] Holland JH. Adaptation in natural and artificial systems. Ann Arbor: University of Michigan Press; 1975.
[34] MATLAB Optimization Toolbox 5 User's Guide. The Math Works, Inc.; 2012.
[35] Şahin AŞ, Kılıç B, Kılıç U. Optimization of heat pump using fuzzy logic and genetic algorithm. Heat Mass Transf 2011;47(12):1553–60.
[36] Sreejaya P, Iyer SR. Optimal reactive power flow control for voltage profile improvement in AC–DC power systems. In: Power Electronics, Drives and Energy Systems (PEDES) 2010 Power India; 2010. p. 1–6.
[37] Taghavi R, Seifi A. Optimal reactive power control in hybrid power systems. Electr Power Compon Syst 2012;40(7):741–58.
[38] Lin YZ, Cai ZX, Mo Q. Transient stability analysis of ac/dc power system based on transient energy function. In: Electric Utility Deregulation and Restructuring and Power Technologies (DRPT) 2008, Nanjuing; 2008. p. 1103–8.